

# Recent Results from the STOR-M Tokamak

<sup>a</sup>A. Hirose, <sup>a</sup>M. Dreval, S. Elgriw, <sup>b</sup>O. Mitarai, <sup>a</sup>A. Pant, <sup>c</sup>M. Peng ,  
<sup>a</sup>D. Rohraff, <sup>d</sup>A.K. Singh, <sup>a</sup>D. Trembach, <sup>a</sup>C. Xiao

<sup>a</sup>*Plasma Physics Laboratory, Department of Physics and Engineering Physics, University of Saskatchewan, Canada, akira.hirose@usask.ca*

<sup>b</sup>*Institute of Industrial Science and Technical Research, Kyushu Tokai University, Kumamoto, Japan*

<sup>c</sup>*Oak Ridge National Laboratory, Oak Ridge, Tennessee, USA*

<sup>d</sup>*Present address: Dept. of Physics, Utah State Univ., Logan, Utah, USA*

**Abstract.** This paper reports on two recent experiments carried out on the STOR-M tokamak. The first experiment studied the nature of MHD activities based on singular value decomposition algorithm during the improved confinement phase induced by compact torus injection. The typical MHD modes with mode numbers  $m = 2, 3,$  and  $4$  are suppressed during the improved confinement phase. Shortly before the termination of the improved confinement phase, MHD activities reemerge, starting with a gong-mode-like burst followed by oscillations of a rotating  $m = 2$ . The second experiment was successful current start-up with a simulated spherical tokamak configuration where the inner Ohmic heating coils surrounding the iron core are deactivated in STOR-M. Current start-up was also achieved with all the vertical equilibrium field coils deactivated. In the latter case, the vertical equilibrium field was provided solely by the image vertical field produced by the magnetization current in the iron core and compensated for by the current through the feedback control vertical field windings. The observed waveforms agree well with numerical simulations.

**Keywords:** Tokamak, Spherical tokamak, Compact torus, MHD, H-mode, current startup.

**PACS:** 52.55.Fa

## INTRODUCTION

STOR-M is a small iron core tokamak at the University of Saskatchewan for basic tokamak physics studies and fusion technology development. Pioneering experiments on alternating current (AC) tokamak operation, plasma heating via a short current pulse, electrode biasing, and compact torus (CT) injection have been performed in the past. In this paper, we present recent experiments and data analyses on the effects of CT injection on the MHD Mirnov oscillations and simulated current start up in an iron core spherical tokamak (ST) using the STOR-M tokamak. Injection of compact tori into a tokamak is a promising technology to deliver fusion fuels directly to the core of a large tokamak fusion reactor [1]. CT is a doughnut-shaped high density plasmoid confined by its own magnetic field, and its rigidity during acceleration to a high velocity has been demonstrated. Disruption-free CT injection into tokamaks has been achieved in several devices [2-4]. During the phase of CT penetration through the tokamak magnetic field, CT acts like a rigid magnetic dipole in the lowest order

approximation and expels tokamak magnetic field lines. When the CT magnetic field reconnects with that in a tokamak plasma, particles in CT are released into the tokamak discharge through the reconnected magnetic field lines. In addition, particle input may also change the pressure profile in the tokamak. Whether fuelling by CT injection excites MHD instabilities is one of the central questions surrounding the technology. Contrary to usual expectations, CT injection into STOR-M induces improved confinement phase and suppressed  $m = 2$  Mirnov oscillations. However,  $m = 3$  Mirnov oscillations are not noticeably affected by CT injection [4]. Since the  $m = 2$ , and  $m = 3$  Mirnov coils used in previous experiments picked up only one particular mode and the digitizer with 8-bit resolution did not allow more detailed analyses of the MHD modes. In recent experiments, 12 Mirnov coils evenly distributed in the poloidal direction have been installed and data are collected using 14-bit digitizers. This allowed more detailed analyses of the poloidal MHD modes,  $m$ , in STOR-M discharges and the effect of CT injection on those modes.

Plasma current start-up is one of crucial issues in a spherical tokamak (ST) reactor which has limited space at the center for transformer magnetic flux. The component test facility (CTF) is a proposed nuclear component testing facility, which provides data for ITER and Demo reactors. To overcome the difficulty in current start-up in an ST, use of an iron core with a small radius has been proposed for initiating the plasma current up to 380 kA in CTF [5]. As the iron core is eventually saturated during the ramp-up of the plasma current up to 16 kA, it becomes an air core transformer after saturation.

Plasma equilibrium during the transition from the unsaturated to saturated phase should be carefully controlled. As the vertical magnetic field created by the image field by the iron core disappears during the core saturation phase [6-8], a vertical field and transformer flux must be carefully supplied, which needs detailed numerical and experimental studies. A couple of operation scenarios can be considered for initial plasma current start-up in the unsaturated phase in CTF with an iron core.

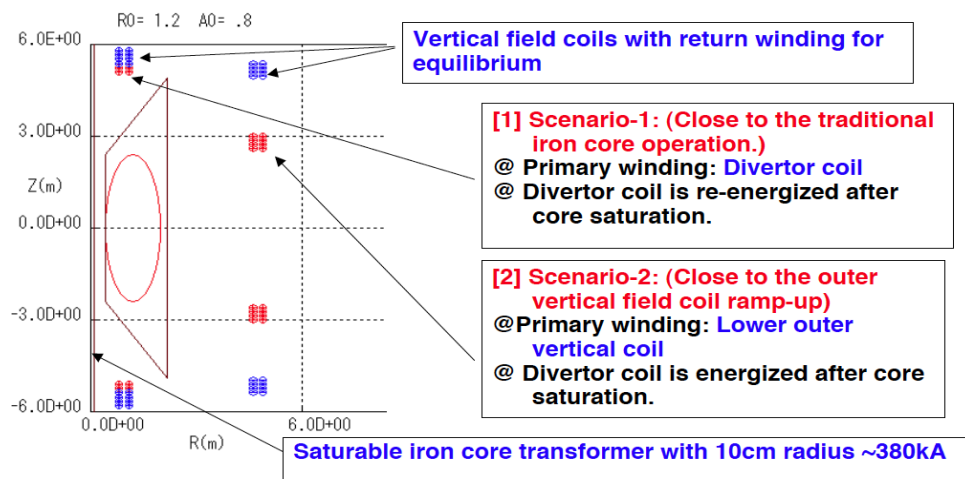


**FIGURE 1.** CTF PF coil layout for iron core operation.

The poloidal field (PF) coil layout is shown in Figure 1. The first scenario is to use the divertor coil as a primary winding. As this operation is close to the traditional iron core operation, no experimental verification will be necessary. The vertical field coil should have a return winding to avoid excitation of the iron core.

The second operation scenario is to use the outer and lower vertical field coil in CTF as a primary winding. The outer and upper vertical field coil with the return winding is used for equilibrium as well. In this study we try to start a plasma current using this second operation scenario. The present poloidal coil layout in CTF does not need extensive modification from the present arrangement. In the study presented in this paper, the outer Ohmic heating (OH) coils in STOR-M tokamak are used to simulate current start up in STs based on the second scenario.

## EXPERIMENTAL SETUP

Figure 2 (a) shows the cross-section of the STOR-M tokamak ( $R = 46$  cm,  $a = 12$  cm,  $B_t = 1$  T,  $I_p \leq 40$  kA). The Ohmic heating (OH) coils consist of 8 turns: 4 inner turns wrapping around the central iron core of 0.32 m in diameter and 4 outer turns with a larger diameter of 1.7 m. The vertical equilibrium (VE) coils consist of 2 outer turns of a diameter of 1.7 m and 2 inner turns of return windings, also wrapping around the iron core. The necessary vertical field required for equilibrium is provided partly by the current through VE coils and partly by the image vertical field due to the iron core, with the balance provided the feedback coils (FB) for horizontal position control. Various poloidal field windings in the STOR-M can be disconnected without major efforts

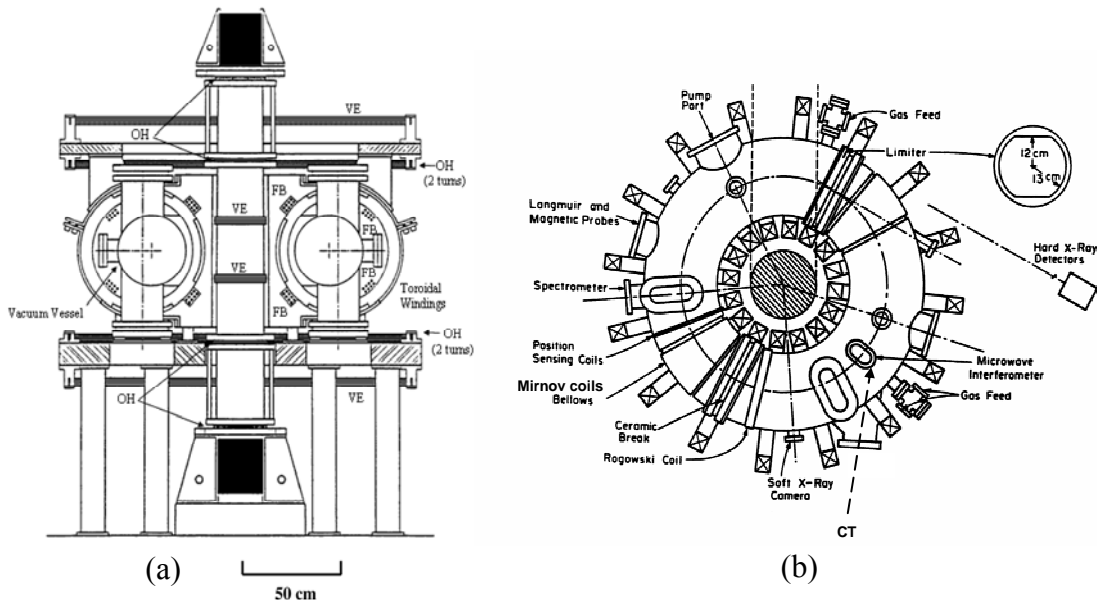


Figure 2. STOR-M layout

Figure 2 (b) shows the top view of STOR-M with ports marked for various diagnostics. CTs are injected through the tangential port shown in the diagram. 12 discrete Mirnov coils evenly distributed poloidally outside a thin bellows at poloidal

angles ( $\theta_i = (2i+1) \times 15^\circ$ ,  $i = 0, \dots, 11$ ), with  $\theta = 0^\circ$  located on the outer mid-plane of the vacuum vessel, are used to measure the fluctuating poloidal magnetic field,  $dB_0/dt$ , resulting from all MHD modes. The Singular Value Decomposition (SVD) technique [9] is used to analyze the MHD signals with the poloidal mode numbers  $m$  up to 6.

## EXPERIMENTAL RESULTS

### Effects of CT Injection on the MHD Fluctuations

Figure 3 shows the waveforms of a STOR-M discharge with a CT injected at  $t = 15$  ms during the current flat-top phase. CT injection induced a significant increase in electron density ( $\bar{n}_e$ ), reduction in  $H_\alpha$  radiation intensity, increase in global energy confinement time ( $\tau_E$ ), and reduction of the  $m = 2$  Mirnov oscillations and floating potential fluctuations ( $\Phi_f$ ). CT injection did not cause visible changes in plasma current ( $I_p$ ), loop voltages discharge ( $v_l$ ), or  $m = 3$  Mirnov oscillations (not shown). The waveforms clearly suggest that CT injection induced a transient improved confinement (H-mode) phase for about 4 ms. It has also been noticed that the amplitude of  $m = 2$  Mirnov oscillations returned to a higher level before the termination of the improved confinement phase, raising a question whether the increase in  $m = 2$  Mirnov oscillations is a direct or indirect precursor for the H-L back transition in STOR-M.

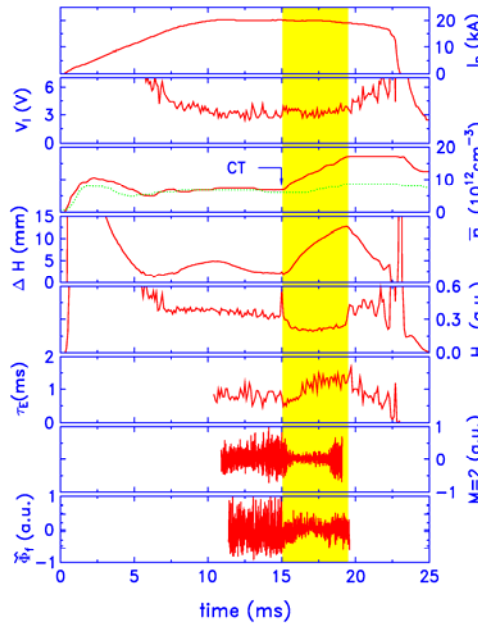


**FIGURE 3.** STOR-M discharge waveforms during a discharge with CT injection.

Figure 4 shows the MHD oscillations measured by one of the 12 Mirnov coils during a more recent CT injection experiment. In this discharge, a CT was injected at  $t = 15.25$  ms. CT injection caused a phase of about 1 ms with suppressed MHD

oscillations. SVD analyses show that the dominant MHD modes are  $m = 2$ ,  $m = 3$ , and  $m = 4$  modes before CT injection. SVD analyses during the MHD suppression phase (15.8 - 16.2 ms) did not reveal clear mode structures since MHD oscillations are suppressed by CT injection to nearly the noise level. The suppression phase is terminated by a spike in the Mirnov signal followed by coherent oscillations.

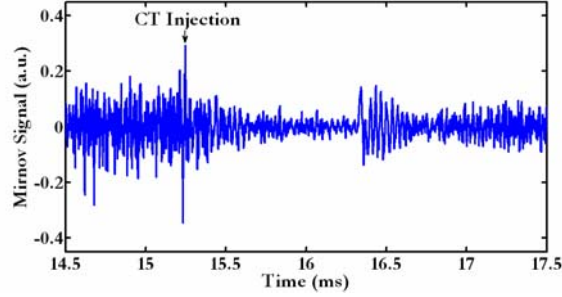


**FIGURE 4.** Mirnov oscillations.

Figure 5a shows a contour plot of the Mirnov raw signals near the time when the MHD oscillations reappear. Figure 5b is a screw-like 3D representation (axial coordinate: time, azimuthal coordinate: poloidal angle, radial coordinate: signal amplitudes with color codes) suggesting helical motion of certain magnetic island. Both plots point to a rotating  $m = 2$  structure.

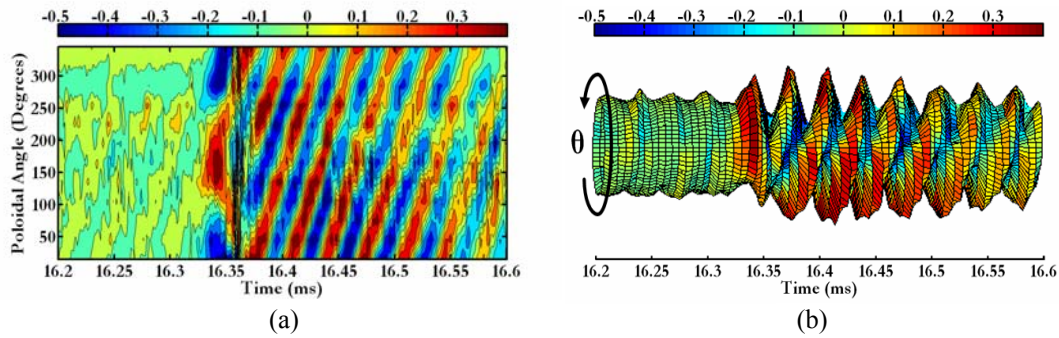


**FIGURE 5.** Mirnov raw signals in contour plot and 3D plot.

To study the details of the MHD oscillations during the reoccurrence phase, SVD analyses have been performed for the time window between 16.2 ms and 16.6 ms. The diagram on the left hand side in Fig. 6 is the polar plot of the space vectors (Principal Axes, PA) of the first two dominant modes.

This polar plot clearly reveals the  $m = 2$  double magnetic islands structure. On the right hand side, the corresponding time vectors (Principal Components, PC) represents the oscillating waveform resulted from the rotation of the principal axis of the spatial structure (seen by a fixed probe). The frequency of the oscillations is about 30 kHz.

These two components represent sine and cosine parts of the same  $m = 2$  mode. This explains the two similar polar plots with only a rotational difference Fig.6 (a), and also the phase shift in two time vectors (Fig. 6 (b)).

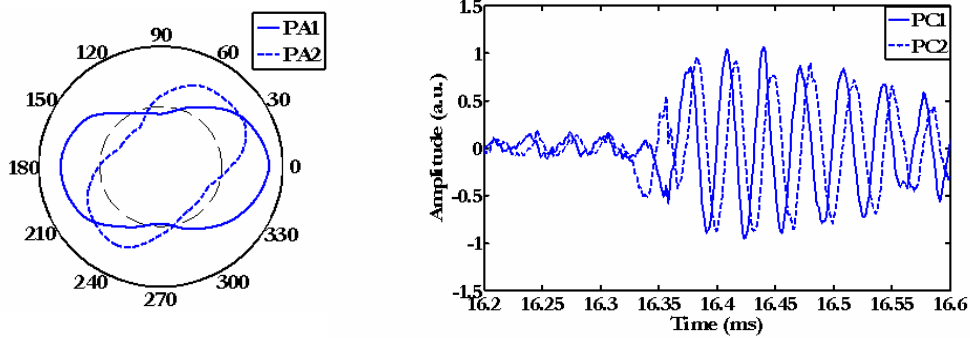


FIGURE 6. Spatial and temporal structure of the magnetic island ( $m=2$  pair).

The third dominant mode revealed in SVD analyses is unpaired. The spatial structure of this mode belongs to  $m=1$  mode with very distinct time evolution as it is shown in Fig. 7. The plot of temporal evolution shows that the  $m=1$  mode appears suddenly at 16.34 and vanishes at 16.4 ms. This mode does not have the usual properties of a traveling wave because it does not propagate nor grow (and decay) gradually as the  $m=2$  mode as shown in Fig. 6.

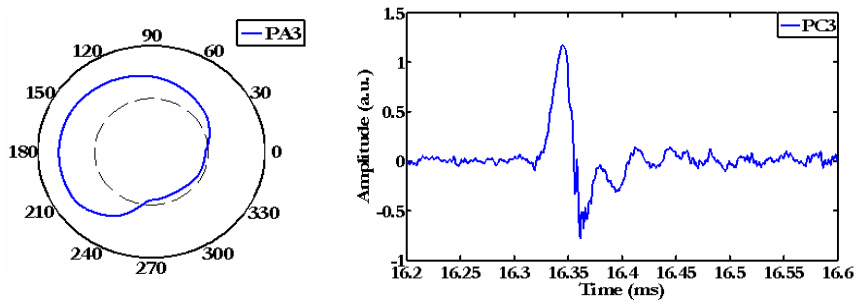
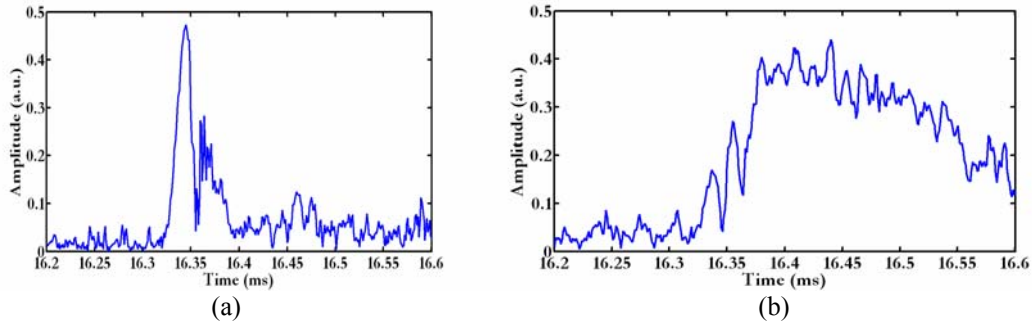


FIGURE 7. Spatial and temporal structure of the  $m=1$  gong mode.

This bursting  $m=1$  mode is of the characteristics of the gong mode observed earlier in the JET tokamak [10]. The gong mode maybe rotates poloidally and toroidally like any other MHD modes. However, its lifetime is shorter than the rotation period which explains why gong mode appears as a lone mode without its companion in SVD analyses. The gong mode has also been reported with different mode numbers in some large tokamaks such as JET and Tore Supra [11] where different methods have been used to analyze Mirnov signals.

Figure 8 (a) and (b) show the evolution of the  $m=1$  gong mode and the magnetic island  $m=2$  based on direct calculation of spatial Fourier components [10] using all 12 raw probe signals. Previous studies indicate that the gong mode is caused by sawtooth crashes in the  $q=1$  core region [12]. The figure clearly shows that the gong mode preceded the  $m=2$  mode. Currently, a soft x-ray (SXR) diagnostic system is under development for the STOR-M tokamak to investigate the possible relationship between the gong mode feature of the MHD fluctuations and the sawtooth activities as well as their relationships to CT injection.



**FIGURE 8.** Mode evolution of MHD modes. (a) the  $m=1$  gong mode, and (b) the  $m=2$  mode.

## Simulation of Plasma Current Start-up by Outer Vertical Field Coils in an Iron Core ST

The feasibility of the proposed second scenario for current start-up was first tested numerically by the plasma circuit equations [6] and experimentally verified in the iron core STOR-M tokamak. The normal plasma current in STOR-M is  $\sim 20$  kA, which is driven by the inner OH coils (4 turns) wound on the iron core and the outer OH coils (4 turns).

To simulate the current start-up of an ST in STOR-M, the inner OH coils were deactivated, and the outer OH coils (corresponding to the outer vertical field coil in CTF) were used as a primary winding as shown in Fig. 9 (a). Furthermore, the vertical equilibrium coils can be also deactivated with a layout shown in Fig. 9 (b), to achieve current start-up. Using the parameters of the PF coil layout-1 shown in Fig. 9 (a), current start-up in the ST for the second operation scenario was calculated with the outer OH coil and vertical field coil for the STOR-M geometry. Figure 10 shows the simulated waveforms of the plasma current and vertical fields. The plasma current is 10 kA.

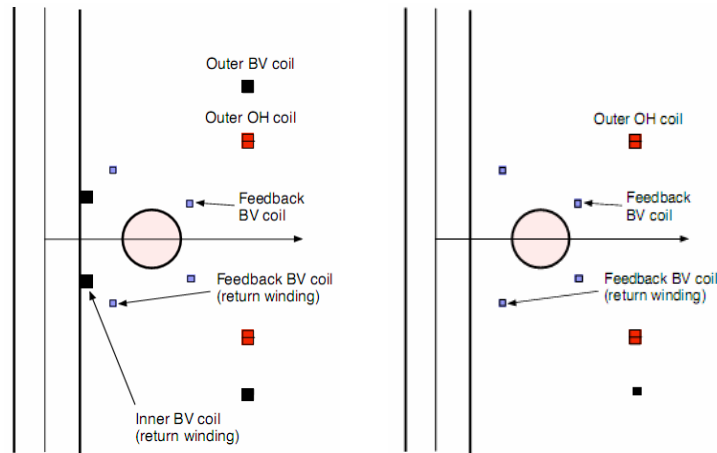


**FIGURE 9.** (a) ST simulation for the second operation scenario in STOR-M. (a) PF coil layout-1, (b) PF coil layout-2.

The initial vertical field before breakdown by the bias current of 73 A of the iron core transformer is as small as +1.9 Gauss, which does not affect the plasma breakdown. The externally applied vertical field is slightly larger than the

equilibrium field during discharge as seen in Figure 10. It can be compensated for by the feedback control vertical field.

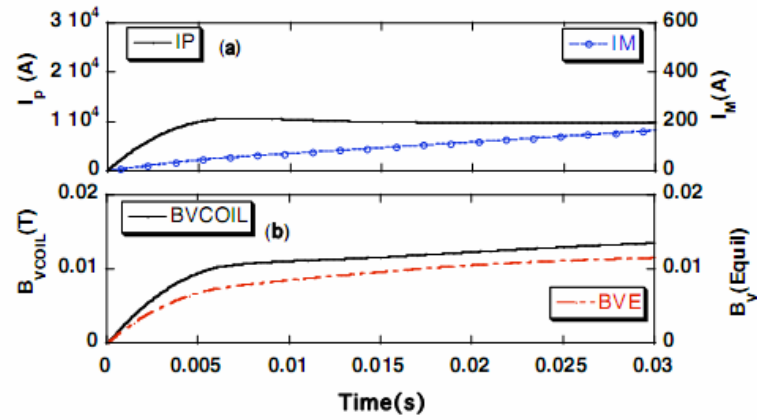


**FIGURE 10.** Numerically calculated current waveforms in the ST simulation PF coil layout-1 in STOR-M. (a) Plasma current (IP) and the magnetizing current (IM), (b) externally applied vertical field (BVCOIL) and equilibrium vertical field (BVE).

Based on this numerical simulation, discharge experiments have been conducted with outer OH coils. The plasma breakdown was obtained from the first shot and the plasma current was increased to  $\sim 11$  kA shot by shot through discharge cleaning as shown in Figure 11. The obtained plasma current waveform is similar to the simulation shown in Figure 10 and discharges are reproducible.

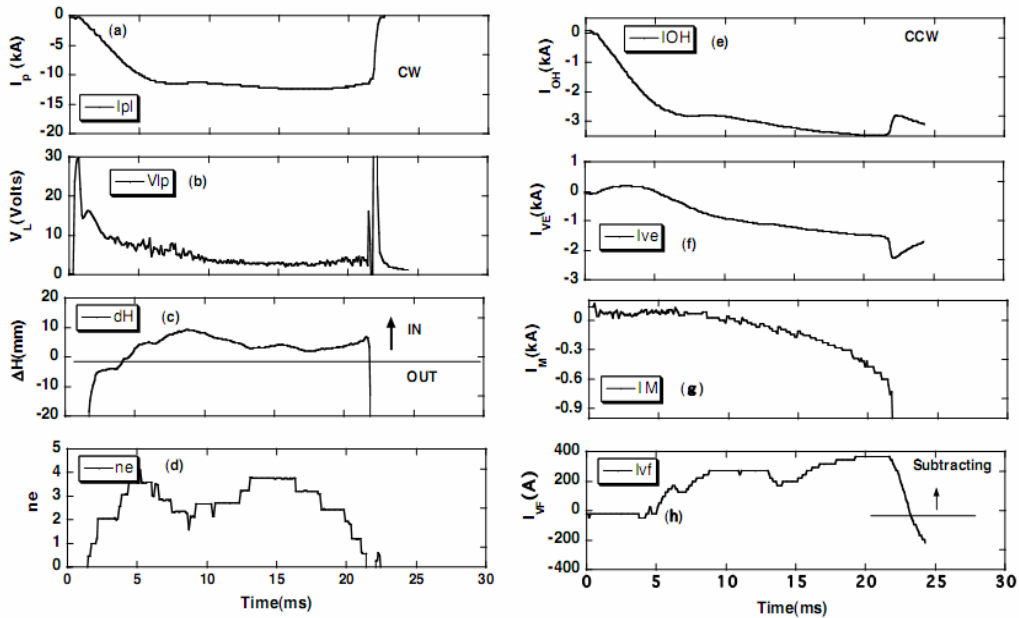


**FIGURE 11.** Experimentally observed current waveforms in the ST simulation (PF coil layout-1) in STOR-M. (a) plasma current, (b) loop voltage, (c) plasma position, (d) the line average density, (e) the outer OH coil current, (f) vertical coil current, (g) magnetizing current in the iron core, and (h) feedback coil current.

Finally, the vertical equilibrium coil was also deactivated and vertical field coil for feedback position control was used for equilibrium, in addition to image vertical field. Although this is a very simple coil layout, very reproducible discharges were also obtained as shown in Figure 12.

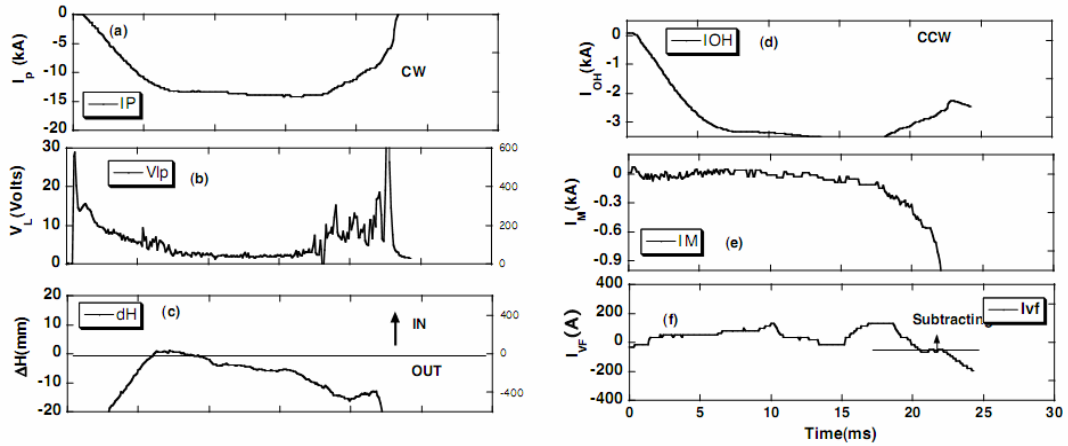


**FIGURE 12.** Experimentally observed waveforms in the ST simulation (PF coil layout-2) in STOR-M. (a) Plasma current, (b) loop voltage, (c) plasma position, (d) the outer OH coil current, (e) magnetizing current in the iron core, and (f) feedback coil current.

It has been found in this study that the plasma current can be started up by the outer vertical field coil in an iron core tokamak without any application of external heating power. The Ohmic primary windings in an iron core tokamak can be placed anywhere, because the stray field from the iron core during the magnetically biasing phase is very small due to the small bias current and it does not affect the breakdown. Therefore, the poloidal coil layout in an ST reactor can be determined by the iron core saturation phase. Saturable iron core operation should be further demonstrated experimentally before this scenario can be applied to CTF.

## SUMMARY

MHD instabilities in STOR-M tokamak have been measured by a poloidal set of 12 discrete Mirnov coils with a focus on the H-mode phase induced by CT injection. MHD activities are suppressed during the transient H-mode phase and reemerge prior to the H-L back transition. Singular value decomposition analyses reveal that the MHD oscillations restarted with the short-lived  $m=1$  gong mode followed by a rotating  $m=2$  mode.

The iron core STOR-M tokamak has been used to simulate iron core spherical tokamak (ST) current start-up using vertical field coils. Reproducible current start-up up to 10 kA has been realized by deactivating the inner ohmic heating coils in STOR-M, leaving the outer ohmic heating coil alone to simulate the vertical field coils in an ST, and by further deactivating the vertical equilibrium coils. In the latter case, the main vertical equilibrium field was supplied by the image vertical field due to the magnetization current in the iron core and the balance of the necessary vertical field was supplied by the feedback vertical fields.

This work has been sponsored by Natural Sciences and Engineering Council (NSERC) of Canada and the Canada Research Chair (CRC) Program.

## REFERENCES

1. Parks, P. B., Phys. Rev. Lett. **61** (1988) 1364.
2. Raman, R., et al., Phys. Rev. Lett. **61** (1994) 3101.
3. Nagata, M., et al., Nucl. Fusion **45** (2005) 1056,
4. Sen, S., Xiao, C., Hirose, A., et al., Phys. Rev. Lett. **88** (2002) 18501.
5. Mitarai, O., Peng, M., et al., "Analysis of Plasma Current Ramp-up and Ignition in CTF", to be submitted.
6. Mitarai, O., Wolf E, S. W., Hirose, A., Skarsgard, H. M., Plasma Phys. Control. Fusion **27** (1985) 395.
7. Mitarai, O., Hirose A., Nucl. Fusion **24** (1984) 481.
8. Mitarai, O., Hirose, A., Journal of Fusion Energy **4** (1985) 395.
9. Nardone, C., Plasma Phys. Control. Fusion **34** (1992) 1447.
10. Duperrex, P. A., Pochelon, A., Edwards, A. W., Snipes, J. A., Nucl. Fusion **32** (1992) 1161.
11. Dudok De Wit, T., Lima, R., Pacquet, A.-L., et al., Phys. Plasmas **1** (1994) 3288.
12. Dong, Y.B., Pan, C.H., Liu, Y., Fu, B.Z., Plasma Sci. Technol. **6** (2004) 2307.